NASA
Technical Memorandum 79003

AVRADCOM
Technical Report 78-47

(NASA-TM-79003) WEAR OF SEAL MATERIALS USED IN AIRCRAFT PROPULSION SYSTEMS (NASA) 30 p
HC A03/MF A01 CSCL 11F

N79-12204

Unclas
G3/26 38003

WEAR OF SEAL MATERIALS USED IN AIRCRAFT PROPULSION SYSTEMS

Robert C. Bill
Propulsion Laboratory
AVRADCOM Research and Technology Laboratories
and
Lawrence P. Ludwig
Lewis Research Center
Cleveland, Ohio

TECHNICAL PAPER to be presented at the
Materials and Processing Congress
sponsored by the American Society for Metals
Philadelphia, Pennsylvania, November 7-9, 1978

WEAR OF SEAL MATERIALS USED IN AIRCRAFT PROPULSION SYSTEMS

by Robert C. Bill
Propulsion Laboratory
AVRADCOM Research and Technology Laboratories
and
Lawrence P. Ludwig
Lewis Research Center
Cleveland, Ohio

ABSTRACT

The various types of seal locations in a gas turbine engine are described, and the significance of wear to each type is reviewed. Starting with positive contact shaft seals, existing material selection guidelines are reviewed, and the existing PV (contact pressure X sliding velocity) criteria for selecting seal materials are discussed along with the theoretical background for these criteria. Examples of wear mechanisms observed to operate in positive contact seals are shown. Design features that can extend the operating capabilities of positive contact seals, including pressure balancing and incorporation of hydrodynamic lift are briefly discussed. It is concluded that, despite the benefits arising from these design features, improved positive contact seal materials from the standpoint of wear, erosion and oxidation resistance will be necessary for further improvements in seal performance and durability, and to meet stringent future challenges. Materials used in noncontacting gas path seal applications are described, and a review of wear studies performed on these materials is presented. Factors that promote drastic changes in the structure and wear behavior of highly porous gas path seal materials are discussed. For low porosity metallic gas path seal materials a correlation between wear characteristics and a factor that includes material strength, ductility, specific heat and hot-working temperature is proposed.

E-9789

INTRODUCTION

In a modern aircraft gas turbine engine there is a multitude of seal locations as shown in Fig. 1, all of which are significant with respect to the performance and reliability of the engine. The types of seal locations may be classified into 2 broad categories.

First there are the mainshaft seals. The primary function of these seals is to protect the bearing compartments from the potentially damaging engine environment outside the compartment. Generally positive contact seal designs are used in the mainshaft seal locations, though sometimes noncontacting labyrinth seals may be employed.

The second type of seal location includes the nominally noncontacting gas path seals. Among the gas path seals are the numerous labyrinth seals designed to reduce loss of high pressure gas from the engine cycle, control cooling air flow through the hot section of the engine, and to maintain pressure balance on the rotor shaft system. Also included among the gas path seal positions are the important outer gas path seal locations over compressor and turbine blade tips. The outer gas path seals are intended to maintain close operating clearance between the rotating blade tips and the stationary seal components, thereby helping to maintain engine efficiency.

Wear of the materials comprising the various types of seals is a very important consideration. Besides directly affecting seal component life, wear and associated loss of seal performance in mainshaft seals can lead to accelerated bearing failure. Also, loss of oil through excessive seal leakage can cause fouling of the primary engine components, promoting stall and presenting severe safety hazards. A study performed on several small military engines showed that a leading cause of early engine removal was oil leakage through mainshaft seals (1), attributable in part to wear of the seal elements.

Though they are not intended to rub during operation, engine structural distortions, thermal response effects, and dynamic loads inevitably lead to transient rub interactions between gas path seal components. If all of the wear incurred during such rub interactions were restricted to the stationary gas path seal material, an overall benefit in terms of reduced operating clearance may be realized, as illustrated in Fig. 2. The efficiency benefits of operating with optimum gas path seal clearances throughout the engine are summarized in (2). Briefly, (2) indicates that a $2\frac{1}{2}$ percent improvement in TSFC (Thrust Specific Fuel Consumption) can be realized with a nominal reduction in gas path seal operating clearances. In addition, wear to the tips of high pressure turbine blades can initiate sites of rapid corrosive attack to the blade through disruption of protective blade coatings. In the compressor, rapid heating of titanium alloy blade tip during adverse rub interactions can potentially lead to severe thermal damage.

Having illustrated the overall significance of wear considerations in gas turbine sealing, it is the intent of this paper to summarize the state of seal material technology particularly from the wear standpoint. Methods of testing, currently used materials, and the current understanding of seal wear phenomena are reviewed. Areas needing further development are suggested.

MAINSHAFT SEALS

General Description

Two types of positive contact mainshaft seals are shown in Fig. 3, and a rather thorough discussion of the operating principles of each may be found in (3). The sealing elements of the face seal design include a rotating seal seat, usually with a hard metallic contact surface mounted to the shaft, and a nonrotating primary seal ring, usually a carbon graphite material, which is allowed to move axially, accomodating axial motion of the seat due to run-out or misalignment. Carbon graphite is chosen as the ring material partly because of its inherent self-lubricating capabilities. Also, a secondary seal is provided between the primary ring carrier and stationary seal housing. Seal closing force is usually provided by a combination of spring force and controlled pressure loading.

The circumferential seal also depicted in Fig. 3, consists of overlapping circumferential segments, usually carbon graphite, held into close proximity to the shaft by means of a circumferential garter spring. Pressure loading of the circumferential seal elements against the rotating shaft is inherently not as controllable as for the case of the face seal design, therefore circumferential seals are generally used in lower differential pressure application than shaft seals. Circumferential seals are able to accomodate greater axial movement between the seal surfaces than face seal however.

Materials

Current materials used in the contacting elements of shaft seals are summarized in Tables I and II, taken from (4), for face seals and circumferential seals respectively. Selection of a specific material combination requires detailed consideration of such things as the seal application severity (expressed as a PV factor, discussed later), the lubricating capacity of the sealed fluid, the presence of erosive debris, and temperature of the seal environment. Also, it should be recognized that "carbon-graphite" denotes a class of materials. Depending on the exact constituents comprising the carbon graphite material, and the processing steps followed in its manufacture, a wide range of mechanical properties may be obtained, as illustrated in Table III (5). Usually in aircraft engine applications the seat material is a hardened martensitic stainless steel (400 series), or chrome plate applied to a shaft material substrate. The intent in this choice of seat material is to reduce erosive wear to the rotating component as fine abrasive particles entrained in the engine air may be carried between the seal elements.

Though applied only with a host of qualifiers, a general guideline in assessing severity of a seal application and suitability of a particular material selection is the PV factor. The PV factor is defined as the product of seal contact pressure in psi and sliding velocity in feet per second. PV ratings for a number of contact seal materials are shown in Fig. 4, taken from (6). It is shown in (7) how the PV rating may be interpretted as a thermal limitation of the seal material, or as a wear criterion. For either interpretation, application of a PV rating must include careful consideration of the seal geometry and surroundings (ability of the seal to dissipate heat) and the likely lubrication mode effective in the seal gap.

Three modes of lubrication that are encountered in contact seals are summarized in Fig. 5 (8). The lubricating fluid is of course the sealed fluid. In fact, at any instant, more than one mode may be operating at various locations in a seal. From the standpoint of reducing wear, it is desirable to operate in the full film lubrication mode. Factors that tend to stabilize the full film mode are surveyed in (9) and include waviness of the seal element surfaces, certain types of angular misalignment, and the formation of a liquid to vapor interface in the seal gap. During seal start-up operations, under conditions of severe misalignment and run-out, and in situations in which lubricant (sealed fluid) supply is not available or lubricant temperatures are high, boundary lubrication or dry sliding modes may be encountered. It is evident that those factors controlling the lubrication mode effective in a positive contact seal are themselves not always very amenable to control.

Wear of Positive Contact Seal Materials

First level screening tests for seal material wear are usually conducted on a fairly simple apparatus, such as the pin-on-disk rig shown in Fig. 6. Here, conditions of sliding speed, contact load, surrounding temperature and environment may be set to simulate those of a selected seal application. Sliding speeds of 100 m/sec are typical for gas turbine shaft seal applications, with nominal contact pressure of several pounds per square inch. Temperatures may exceed 1000° F in severe applications. Usually sliding conditions are dry or in a boundary lubricating mode-obviously it is not possible to simulate full film formation mechanisms on such a rig. Besides pin-on-disk configurations, annular ring configurations or conformal pad geometries are sometimes used in wear testing of seal materials.

An example of the information that can be obtained from such testing is summarized in Fig. 7 (10). Here the effects of variations in carbon graphite material formulations and incorporation of selected additives on sliding wear to the carbon graphite at temperatures to 1200° F are seen. It was concluded that at temperatures to 1200° F, two materials performed satisfactorily: carbon graphite with a carbonized resin impregnant (A-CG-C), and carbon graphite with a metal phosphate impregnant (B-CG-C); all of the other materials underwent accelerated wear combined with rapid oxidation at 1200° F. The 1200° F temperature is in fact approached in some of the more severe aircraft engine contact seal applications. Typical applications are usually at 900° F and lower though.

Besides wear rates and friction measurements, screening tests provide some clues concerning the friction and wear mechanisms operating at seal material interfaces. The ability of carbon graphite to be self-lubricating in the event of dry contact depends on the formation of a thin, oriented, easily shearable layer of graphite on the sliding surface (11). So long as this layer is maintained wear will be low. Certain conditions lead to the disruption of the easily shearable graphite layer. Among them are the thermally induced desorption of adsorbed gases (O_2, H_2O) on the surfaces and edges of crystallites comprising the shear layer (11), and disruption of the surface oxide present on the metal counterface (12). Disruption of the oriented graphitic film exposes the underlying randomly oriented carbon graphite material to sliding contact. The sequence of SEM photographs shown in Fig. 8 illustrates the condition of the carbon graphite sliding surface with the oriented film intact, and various stages of film disruption. It is unclear as to what conditions lead to restoration of the oriented graphite film, possibly from graphitic debris particles (13), and what conditions promote ever more severe sliding wear and higher friction.

An important factor in the high speed sliding contact of seal surfaces is the inherent thermoelastic instability of the contacting geometry. The theoretical basis for this phenomenon is well developed in (14). Briefly, it is shown that any initial nonuniformity in frictional contact may become increasingly exaggerated as local thermal expansion effects lead to ever more concentrated contact effects. Ultimately the entire contact load is supported by a few thermally induced asperities, with wear effects thus concentrated at a few local spots at any instant. Full development of this theory may provide some guidelines for selecting more wear resistant seal material combinations.

Testing of full seal designs or assemblies is usually conducted on a test rig that closely simulates the intended application in terms of bearing compartment design, sealed lubricant, and lubrication system features. It is intended that the seal should operate much as it would in its final installation. Under normal operating conditions, when full or partial film lubrication is present, wear to the contacting seal components is negligible. However, under severe operating conditions as might occur when the lubricant supply is cutoff for some reason, or when the seal is exposed to a high concentration of abrasive material, or excessive runout and vibration is encountered, the sealing elements can suffer severe distress. Besides wear to the carbon graphite seal elements similar to wear effects described previously, the hard metallic seat often shows evidence of severe distress. It is often observed that severe rubbing conditions promote thermocracking or "heat checking" of hard steel seat components, as shown in Fig. 9 for a 440C seal seat. In (15), a PV type criterion is developed, based on thermal shock resistance of seal materials in which it is envisioned that rub induced heating leads to thermal stresses exceeding the strength of the seal material. The significance of frictional heating on the properties and structure of the 440C material shown in Fig. 9 may be appreciated in the section micrographs of Fig. 10. The thin, light shaded layer adjacent to the rub surface is believed to be a fully martensitic layer, generated by rapid local thermal cycling under rub conditions. Temperatures in this layer must have reached 1400 to 1500° F, followed by cooling to about 500° F within a few seconds. The depth of this layer roughly corresponds to the depth of the cracks shown in Fig. 9. At greater depths beneath the rub surface, a soft darker shaded region is encountered in which lower than bulk hardness are measured. Here, frictional heating promoted further tempering of the hardened 440C structure.

Besides wear considerations for the primary sealing elements, there are wear problems associated with the secondary sealing paths of both circumferential and face seal designs. Due to shaft runout effects, low amplitude oscillatory motion can promote fretting damage to the lap joint interfaces of the circumferential seal and the piston ring carrier interface of some face seal designs. The significance that fretting wear can have on leakage through secondary seal component is summarized in (16). Due to fretting damage to the piston ring in an experimental face seal design, thirty to forty percent of the total seal leakage (amounting to several thousand SCFM) was lost through the secondary seal.

Some recent advances in seal design show promise for reducing some of the wear problems discussed here. With careful balancing of pressure forces on the seal primary ring, the contact pressure may be controlled to a low value just sufficient to maintain sealing, thereby effectively reducing the PV factor. Hydrodynamic lift may be provided to the primary seal elements by incorporating lift pads in the seal design (Fig. 11), enabling the seal to run on a thin, stable gas or liquid film under steady state conditions. Even with this self-acting lift feature of course, sliding contact is incurred on start-up and shut-down as well as under conditions of unstable operating geometry. Also, the effects of abrasive particles carried across the primary seal interface are still significant, as is fretting wear to the secondary sealing elements.

In summary, for positive contact mainshaft seals, there is a significant need for improved wear, erosion, and oxidation resistant self lubricating materials for temperatures to 1200° F. Also, hard materials or coatings exhibiting good thermal stability with respect to properties and structure are needed in seal seat applications. The development of several plasma sprayed alloy and cermet materials for mechanical face seal applications is reported in (17). High temperature fretting and abrasion resistant materials are required for secondary seal locations.

GAS PATH SEALS

General Survey

Examples of materials used in both secondary gas path seal locations and in outer gas path seal locations are summarized in Fig. 12. The primary consideration in selection of the seal materials for various locations is the local operating temperature. The desirable wear characteristic of each of the materials indicated in Fig. 12, in their respective locations, is that the seal material should wear rather than the rotating labyrinth seal knife edge or blade tip. In general there are three approaches, presented schematically in Fig. 13, that may be followed to provide a gas path seal material with this desirable wear characteristic often (somewhat misleadingly) called abradability.

The first approach, indicated in Fig. 13(a), is to employ a highly porous low density material. Such materials are usually prepared by sintering metal powders or fiber particles, often in mixture with transient filler materials. It is also possible to plasma spray such a structure by spraying metal particles mixed with easily volitilizable polymeric particles, or with graphite. Abradability is afforded by the easy removal of discrete particles from the bulk seal material; fracture may readily occur across the small interparticle bond area when a rub occurs. Limitations inherent in this type of material include susceptibility to erosion damage, and inefficient sealing due to leakage through open porosity.

A second class of gas-path seal materials depicted in Fig. 13(b), includes more dense structures (less than 30 percent porosity) which are often plasma-sprayed and, in some cases, sintered, hot pressed, or even cast. Rub interactions for this class of seal materials are accommodated in a more complex manner than were those for the first type of seal material. Usually a combination of plastic deformation, material compliance (densification), and machining mechanisms is involved. Again, variations of this type of material are used in gas-path seal locations throughout the engine - elastomeric materials being employed in low pressure compressor positions, low temperature metals in higher compressor stages, and high temperature materials in the turbine.

The third class of gas-path seal materials derives its rub tolerance from the geometric arrangement of thin metal sheets from which the seal is fabricated. Probably the most widely used example of this type is metallic honeycomb. The honeycomb cell walls are oriented in the radial direction. Consequently, very little metal to metal contact surface area is involved when a rub interaction occurs. Honeycomb structures are generally applied to low pressure turbine seal positions.

Methods of Evaluation

Wear characteristics of gas path seal materials are evaluated on test rigs, like the one shown in Fig. 14, that incorporate geometries and rub parameters similar to those encountered in the engine. Rub speeds of up to 320 m/sec (1000 ft/sec), and radial incursion rates of from 2.54 to 254 micrometers per second (0.1 to 10 mils/sec) are typical of the range of controlled parameters investigated. Most rigs have provisions for testing both labyrinth seal knife edge and multiple blade tip rotors. Bulk temperature of the seal material is usually controlled. Seal sample dimensions are usually such that the rub arc length is about 30° or less. Measured parameters include radial and frictional forces, seal material and rotating material wear volumes, pyrometer measurements of rotor temperatures, and thermocouple measurements of seal material temperatures. Also, debris from the rub zone is often collected for analysis, and seal and rotor samples are generally subjected to metallographic study. Wear performance or abradability is usually summarized as a volume wear ratio number, the wear volume measured on the rotor divided by the wear volume of seal material.

It is very difficult to assess the extent to which various seal rub test rigs simulate engine seal rubs. Comparisons can only be made on the basis of the appearance of rubbed seal and blade tip (or knife-edge) surfaces upon engine overhaul or rework inspections. Part of the difficulty lies in the great amount of uncertainty as to the exact conditions under which engine rubs occurred. Also, the effects of rub interactions on seal and rotating component surfaces are usually masked by erosion and oxidative effects that can alter the appearance of the rubbed surfaces. Nevertheless, seal rub tests from what are probably (from the standpoint of seal studies) the most controlled engine tests reported do show general material ranking trends similar to those obtained from rig tests (18).

The most open questions concerning the similarity between rig tests and engine rub conditions probably relate to the blade tip test geometry. The significance of nominal blade pass frequency, theoretical chip or cut depths per blade (incursion rate divided by blade pass frequency) and seal rub arc length are not well understood.

Wear Phenomena

Low density materials. - For low density gas path seal materials, the intent is that rub interaction be accommodated by removal of discrete particles, thereby minimizing frictional heating effects and wear to the rotating component. Under some rub conditions however, it is observed that the surface of the low density seal material becomes smeared, and in effect the rotating component is in contact with fully dense seal material. Such a smeared rub surface is depicted in Fig. 15. As indicated in Fig. 16, the rate of frictional heat generation at the rub interface increases by two orders of magnitude when smearing occurs (19). Microsections of a Ti-6Al-4V rotating component after such a high energy rub (Fig. 17) show evidence of very rapid oxidation in some cases as indicated by quasi-spherical cavities in the rub surface and intense white sparking during the rub. Also, in other studies it was observed that high energy rubs promoted fine martensitic platelet formation near the rub surface (20).

Naturally, since the occurrence of smearing has such a marked effect on the rub behavior of low density gas path seal materials, conditions that promote smearing are of interest. For a series of labyrinth seal knife edge tests reported in (21), a general observation was that low incursion rate conditions were more likely to promote smearing than high incursion rate conditions. A model, based on thermal diffusivity effects and summarized in Fig. 18, was proposed to account for this trend. Additional effects, namely particulate escape statistics under various rub conditions and geometries, were studied in (19). A thorough study of the first order effects of the controllable rub parameters (speed, incursion rate, geometry) on rub energy and blade tip wear is reported in (20), with the effect of incursion rate and occurrence of rub surface smearing again being very significant. However, the tendency toward smearing was observed to be greatest under high incursion rate conditions. These apparent disagreements between the results of (20) and (21) are probably attributable to very different test geometries - a rotating knife edge was used in one case (21) and a stationary blade tip, rotating seal material geometry was used in the other case (20).

To summarize the understanding of rub characteristics of low density gas path seal materials, adverse rub surface conditions and some sets of rub parameters that favor those conditions have been identified. It should be pointed out that most of the studies have been performed on one family of sintered fiber low density seal materials. The degree to which results obtained on these materials would apply to other low density seal materials is uncertain. Also uncertain is the exact mechanism or combination of mechanisms responsible for the onset of smearing, with consequent rapid frictional heating and wear to the rotating component.

Dense plastically deformable materials. - The rub behavior of this second class of gas path seal materials is more stable than that of the porous materials since the structure of the material is not so prone to drastic change under rub conditions. The comparative performance of a series of dense seal materials prepared by plasma spray desposition is summarized in Table IV. In all cases rubbing was against Ti-6Al-4V simulated blade tips. The materials were selected on the basis of their being potentially machineable by the titanium alloy blades, hardness versus temperature being a rough first order screening guide. No single material property except perhaps the impact strength correlates with the rub performance ranking summarized in Table IV. However, motivated by considerations of adiabatic heating of the seal material by rub induced deformation until the hot working temperature range is reached, a nondimensional correlating number is proposed:

$$N = (\text{Tensile Strength}) \times (\text{Elongation}) \times \rho C_p \times T_{hw}.$$

In general, the lower this number, the more "abradable" should be the seal material. For most cases in Table IV, materials with low values of N do in fact produce low blade tip wear.

In studying the rub mechanisms associated with fully dense materials (19), it was proposed that the radial or normal load was controlled by plastic indentation considerations. The frictional energy resulting from the rub was then simply the product of this normal load, the coefficient of friction, and the rub velocity. Order of magnitude agreement with knife edge rub data was obtained with this very simple model, and microsections of rub grooves (Fig. 19) are consistent with the plastic indentation model for normal load. Under blade tip rub conditions however, in contrast to knife-edge conditions, the indentation (rub groove) is at least ten times as wide as it is deep, and the rub cannot be entirely accommodated by plastic displacement of material. Some mechanism of micromachining chip or wear particle formation is required. Examples of such particles are to be seen in the rub debris shown in Fig. 20.

In summary, the rub behavior of fully dense materials under conditions like those encountered in gas path seals has not been studied so extensively as that of the low density materials. Preliminary results seem to indicate that the mechansisms operating are quite different under labyrinth seal knife edge and blade tip geometries. In the former case, a continuous plastic indentation model seems to be descriptive; in the latter case, wear particle and machining chip formation under high speed conditions appear to predominate. The process of very high speed wear particle and machining chip formation is certainly a subject that should be further studied.

Honeycomb seal materials. - The third class of gas path seal materials is fabricated from sheets of selected alloy, brazed together to form an open face structure like that shown in Fig. 21. These material structures offer the advantage of better oxidation resistance than the low density materials discussed earlier, because of reduced exposed surface area, and are more abradable (for a given composition) than the fully dense structures. A distinct disadvantage of the honeycomb is the leakage loss suffered through the open face structure (22).

Wear to the rotating component does not appear to be a major problem with honeycomb seals, and their rub performance does not appear to be affected by variations in rub parameters (23). The major factor inducing rotor wear is the presence of braze nodes between the sheets comprising the honeycomb, as shown in Fig. 22, where the honeycomb wall is 2 to 3 times thicker than the nominal sheet thickness. In the case of the test shown in Fig. 22, an interesting feature was observed on the rub surface of the rotating labyrinth seal knife edge. Evidence of extremely localized "hot spots" may be seen, consistent with the wear pattern measured on the knife edge. These "hot spots" are believed to be manifestations of thermoelastic surface instabilities, discussed earlier.

Not very much, perhaps insufficient, emphasis has been placed on rub studies of honeycomb materials. This is partly because, where leakage over blade tips and labyrinth seal knife edges is important or critical, honeycomb seals have been largely replaced with other seal systems. Where they remain, primarily over low pressure turbine stages and low pressure ratio seal positions, minimum clearance is not so critical a factor.

CONCLUDING REMARKS

Materials for positive contact mainshaft seals are well established, the most widely used material combinations being carbon graphite in combination with hardened steel or chrome plate. Thus far, most advance in reducing seal material wear have been realized through design practices such as accurate pressure balancing and the incorporation of self-acting hydrodynamic lift features. Further improvement in the life of positive contact seals will require materials with improved wear, erosion, and corrosion resistance, and improved thermal stability with respect to structure, dimensions, and properties.

A clear need exists for improved understanding of gas path seal wear phenomena, and for improved gas path seal materials throughout the engine. Gas path seal materials must be abradable and at the same time survive a rather severe environment from the standpoints of erosion, corrosion and thermal shock. The significance of basic first order rub parameters and seal material properties needs to be established. Current development emphasis is being put on plasma-spray deposition techniques to provide either low density abradable structures, or easily machineable alloys.

REFERENCES

1. Rummel, K. G.; and Smith, H. J. M.: Investigation and Analysis of Reliability and Maintainability Problems Associated with Army Aircraft Engines. D 210-10571-1, Boeing Vertol, 1973. (USAAMRDL-TR-73-28, AD-772950.)

2. Mahler, F. H.: Advanced Seal Technology. PWA-4372, Pratt & Whitney Aircraft, 1972. (AD-739922.)

3. Zuk, J.: Dynamic Sealing Principles. NASA TM X-71851, 1976.

4. Ruthenberg, M. L.: Mating Materials and Environment Combinations for Specific Contact and Clearance Type Seals. Lubr. Eng., vol. 29, no. 2, Feb. 1973, pp. 58-64.

5. Fechter, N. J.; and Petrunich, P. S.: Development of Seal Ring Carbon-Graphite Materials. (Union Carbide Crop.; NASA Contract NAS3-13211.) NASA CR-121092, 1973.

6. Standard Handbook of Lubrication Engineering. J. J. O'Connor, ed., McGraw Hill Book Co., Inc., 1968.

7. Zuk, J.: Fundamentals of Fluid Sealing. NASA TN D-8151, 1976, p. 80.

8. Ludwig, L. P.; and Greiner, H. F.: Design Considerations in Mechanical Face Seals for Improved Performance. I-Basic Configurations. ASME Paper 77-WA/Lub-3, Nov. 1977.

9. Ludwig, L. P.; and Greiner, H. F.: Design Considerations in Mechanical Face Seals for Improved Performance. II-Lubrication. ASME Paper 77-WA/Lub-4, Nov. 1977.

10. Strom, T. N.; Allen, G. P.; and Johnson, R. L.: Wear and Friction of Impregnated Mechanical Carbons at Temperatures to 1400° F 760° C in Air or Nitrogen. NASA TN D-3958, 1967.

11. Savage, R. H.: Graphite Lubrication. J. Appl. Phys., vol. 19, no. 1, Jan. 1948, pp. 1-10.

12. Bisson, E. E.; Johnson, R. L.; and Anderson, W. J.: Friction and Lubrication at Temperatures to 1000° F with Particular Reference to Graphite. ASME Paper 57-Lub-1, Oct. 1957.

13. Clark, W. T.; and Lancaster, J. K.: Breakdown and Surface Fatigue of Carbons During Repeated Sliding. Wear-Usure-Verschleiss, vol. 6, no. 6, Nov.-Dec. 1963, pp. 467-482.

14. Kilaparti, S. R.; and Burton, R. A.: Pressure Distribution for Patchlike Contact in Seals with Frictional Heating, Thermal Expansion, and Wear. ASME Paper 76-Lub-11, May 1976.

15. Golubiev, A. I.: Thermocracking of Seal Faces in Mechanical Seals. International Conference on Fluid Sealing, 5th British Hydromechanics Research Association (Cranfield, Bedford, England), 1971, pp. A2·9-A2·16.

16. Johnson, R. L.; and Bill, R. C.: Fretting in Aircraft Turbine Engines. 39th Meeting of the Structures and Materials Panel. AGARD CP-161, 1975, pp. 5.1-5.17.

17. Vreeland, D. C.; Miller, B. E.; and Carroll, J.: Development of Materials Resistant to Wear and Corrosion for Mechanical-Face-Seal Applications. NSRDC-4299, Naval Ship Research & Development Center, 1974. (AD-787642)

18. Materials for Advanced Turbine Engines. First Annual NASA Review, Held at NASA Lewis Research Center (Cleveland, Ohio), Feb. 23-24, 1977. Sponsored by Garrett-Airesearch Manufacturing Company of Arizona, NASA Contract NAS3-20073, 1977.

19. Bill, R. C.; and Wisander, D. W.: Friction and Wear of Several Compressor Gas Path Seal Materials. NASA TP-1128, 1978.

20. Laverty, W. F.: Compressor Seal Rub Energetics Study. (PWA-5616, Pratt & Whitney Aircraft; NASA Contract NAS3-20613.) NASA CR-159424, 1978.

21. Bill, R. C.; and Shiembob, L. T.: Friction and Wear of Sintered Fibermetal Abradable Seal Materials. NASA TM X-73650, 1977.

22. Stocker, H. L.; Cox, D. M.; and Holle, G. F.: Aerodynamic Performance of Conventional and Advanced Design Labyrinth Seals with Solid-Smooth, Abradable, and Honeycomb Lands---Gas Turbine Engines. (EDR-9339, Detroit Diesel Allison; NASA Contract NAS3-20056.) NASA CR-135307, 1977.

23. Shiembob, L. T.: Development of Abradable Gas Path Seals. (PWA-TM-5081, Pratt & Whitney Aircraft; NASA Contract NAS3-18023.) NASA CR-134689, 1974.

Table 1. Face Seal Materials

Environment	Seal nose material	Seal seat material
Gas (Air, CO_2, H_2, He, N_2, O_2)	Carbon graphite	Tool steels Chrome plate Tungsten carbide, plate and solids Chrome carbide plate Ceramics 300-stainless steel 400-stainless steel
	Glass-filled PTFE Carbon-filled PTFE (not for H_2 service) (Sodium and fluorine compounds and radioactivity may adversely affect PTFE)	440-C 4140, 4340 Tool steels (hardened) Chrome oxide
Oil	Carbon graphite	Bronze (for few applications Ni-resist Cast iron Ceramic Stellite (hard facing on 316-stainless steel, especially for high pressures and high velocity) Tungsten carbide Malcornized 316-stainless Carbon-filled PTFE Glass-filled PTFE Sintered iron or bronze Nitralloy, hardened Tool steel, hardened SAE-1040 steel Stainless steel (400 series hardened to Rockwell C-50. This is general recommendation as 316-stainless is not hardenable)
	Cast iron	Bronze
	Graphite molybdenum	Bronze

Table 2. Circumferential Seal Materials

Environment	Seal ring material	Shaft material
Gas (Air, CO_2, H_2, He, N_2, O_2)	Carbon graphite	Chrome plate Chrome oxide Ceramic plate Tungsten carbide plate Chrome carbide plate Hasteloys C&F Ni-O-Nel Tool Steels (limited in water service) 400 Stainless steel 300 Stainless steel
	Glass-filled PTFE Carbon-filled PTFE (not for H_2 service)	Chrome oxide 4140; 4340 (not for water service)
	(Sodium and fluorine compounds and radioactivity may adversely affect PTFE)	440-C (55-60 Rc)
	Filled Polyimide resin	400 Stainless steels (48-53 Rc) Chrome plate

Table 3. Composition, Processing, and Properties of Carbon-Graphite Materials

[Binder material, no. 30 medium pitch, except for BG (no binder).]

	CG-HB (high binder)	CG-MB (medium binder)	CG-LB (low binder)	CG-FF (finely chopped fiber added)	CG-BC (B_4C added)	GCRC (graphite-cloth reinforced composite)	BG (boronated graphite)
Filler material (graphite/non-graphite), wt %	80/20	80/20	80/20	[a]80/20	80/20	------------	100/0
Additive	----------	------------	-------------	----------	B_4C	------------	B_4C
Binder level, pph	70	60	45	70	70	------------	
Additive level, parts by weight[b]	----------	------------	-------------	----------	5	------------	7-10
Molding pressure, N/cm^2 (psi)	3465 (5000)	6929 (10 000)	13 858 (20 000)	3465 (5000)	3465 (5000)	------------	------------
Molding temperature, °C	100	100	100	100	100	------------	------------
Density, g/cm^3	1.829	1.786	1.732	1.617	1.84	1.41	1.65
Flexural strength, N/cm^2 (psi)	2630 (3810)	2310 (3350)	1260 (1830)	2020 (2930)	4430 (6430)	9600 (15 000)	~1400 (~2000)
Elastic modulus, MN/cm^2 (psi)	1.2 (1.7×10^6)	1.1 (1.6×10^6)	0.97 (1.41×10^6)	1.02 (1.48×10^6)	1.78 (2.58×10^6)	1.85 (2.7×10^6)	------------
Hardness, R_S	106	98	84	76	96	------------	------------

[a]Graphite fibers.
[b]Per 100 parts of filler material.

Table 4. Comparison of Performance and Properties of Fully Dense Plasma-Sprayed Seal Materials

	Al	Cu	Cu-10 a/o Zn	Cu-5 a/o Al	Cu-10 a/o Al	Ni-13 a/o Cr
Hardness MN/m^2 (annealed)	196	539	480	843	990	15[illegible]
Tensile strength (10^3 psi) (annealed)	13	32	38	65	65	78
Elongation (% for 2 in. length)	45	55	50	55	28	20
Density (gm/cc)	2.70	8.96	8.80	8.17	7.58	8.62
Specific height (cal/gm °C)	0.215	0.092	0.090	0.099	0.104	0.104
Impact strength (Izod) (ft-lb)	10-15	30-40	30		10-15	
Hot working range (°F)	950	1600	1600	1600	1695	2200
Stacking fault energy ($ergs/cm^2$)	200	40-70	36	4	2	
Meas. blade[a] Tip wear (in.)	0.001 .001	0.026 .038	0.026 .022	0.022 .047	0.014 0.26	0.013 .015
N[b]	0.37×10^6	2.8×10^6	2.6×10^6	2.9×10^6	1.8×10^6	2.2×10^6

[a]Top number refers to room temperature test; lower number to 900° F test.
[b]N = (Tensile Strength) × (Elongation) × ρC_p × T_{hw} where T_{hw} = hot working temperature.

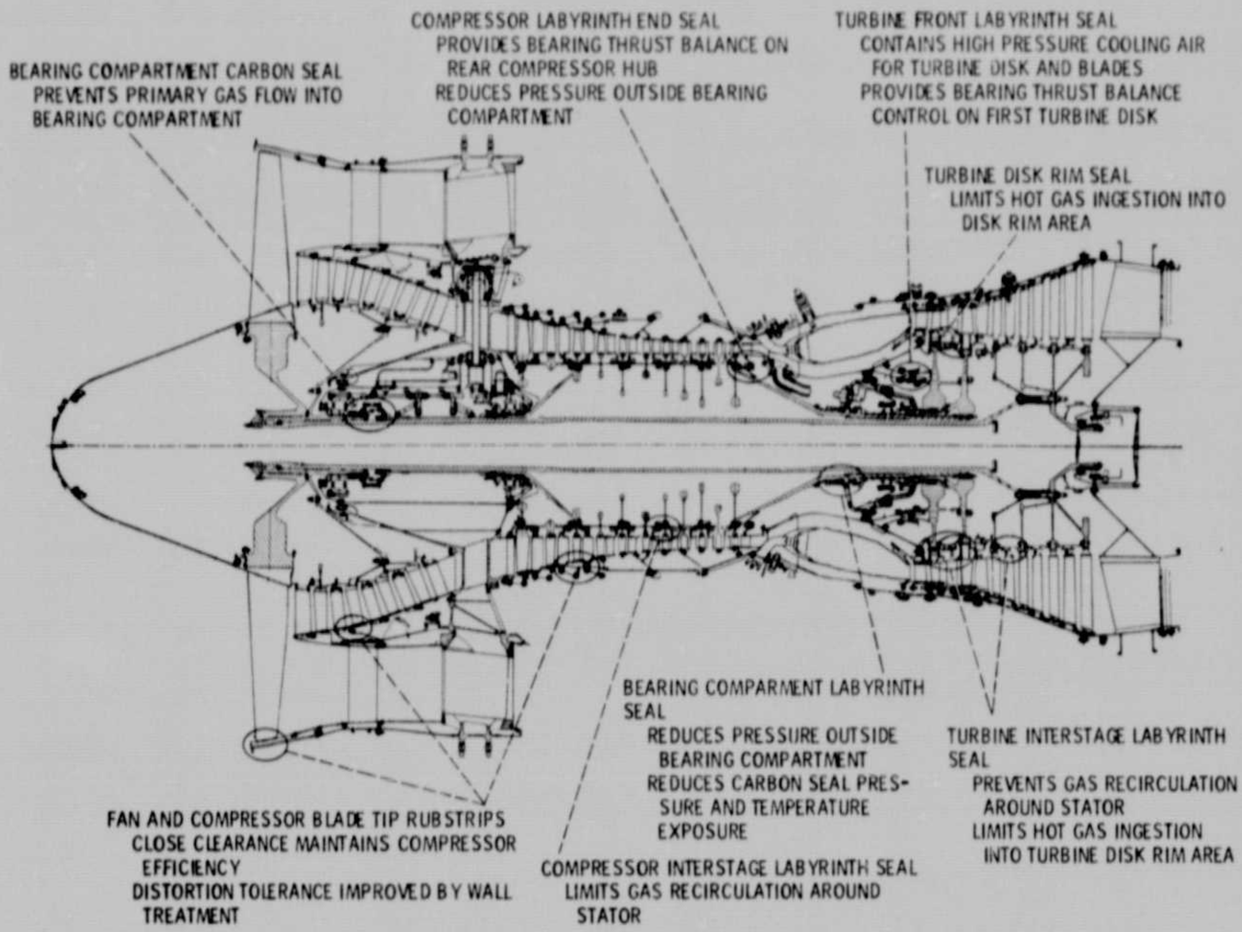

Figure 1. - Modern transport engine (from ref. 2).

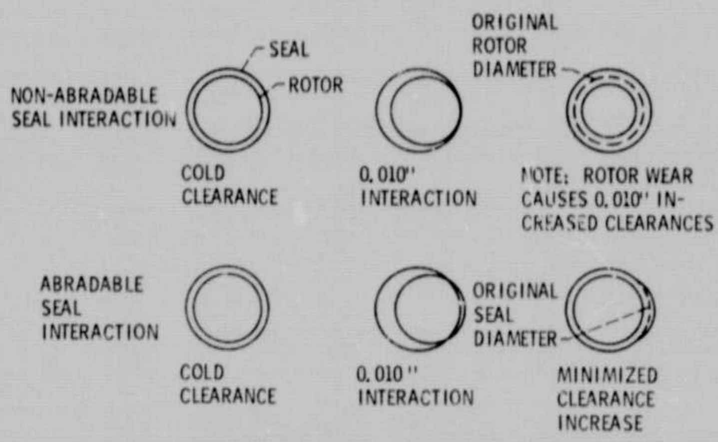

Figure 2. - Effects of rub interactions on gas path seal clearances.

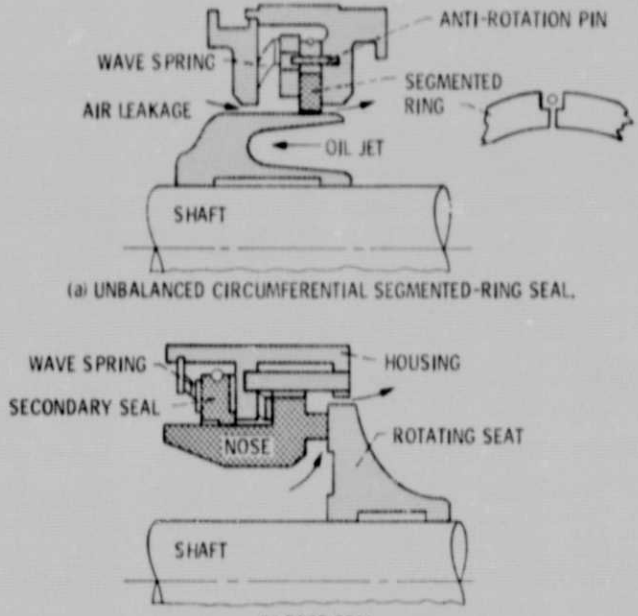

Figure 3. - Conventional shaft seals (ref. 5).

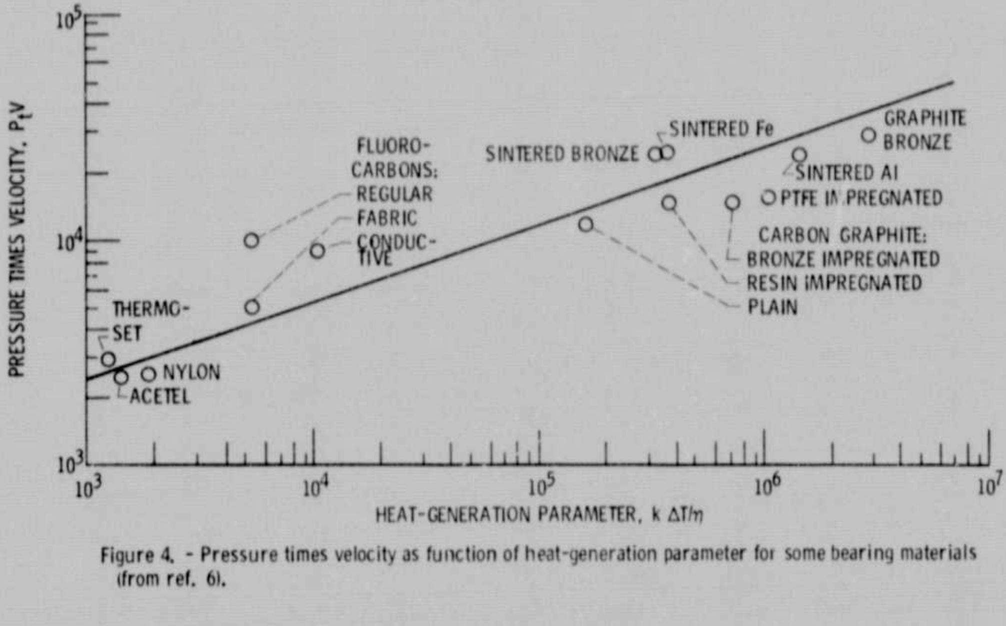

Figure 4. - Pressure times velocity as function of heat-generation parameter for some bearing materials (from ref. 6).

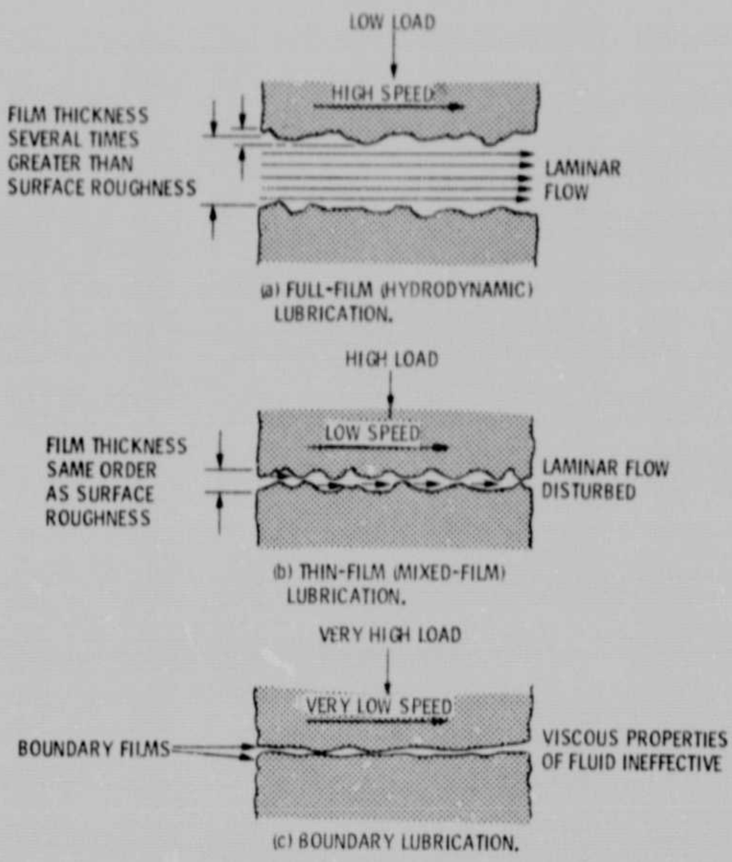

Figure 5. - Hydrodynamic, thin-film, and boundary lubrication modes.

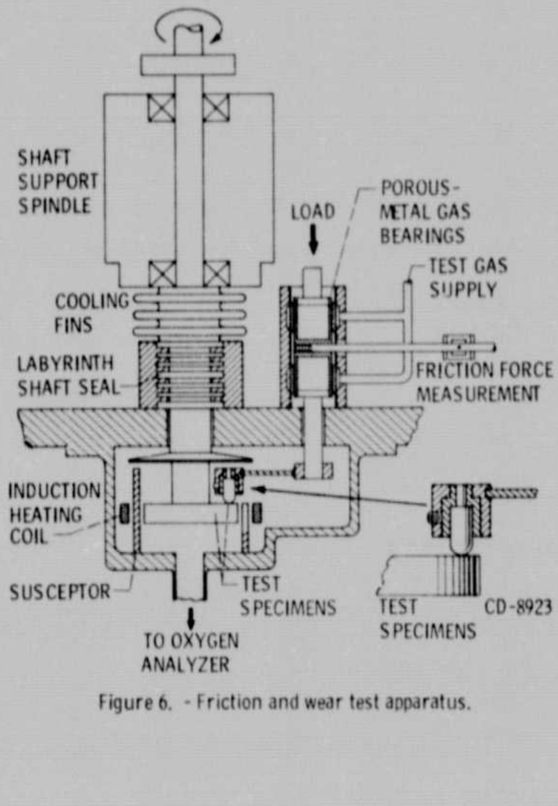

Figure 6. - Friction and wear test apparatus.

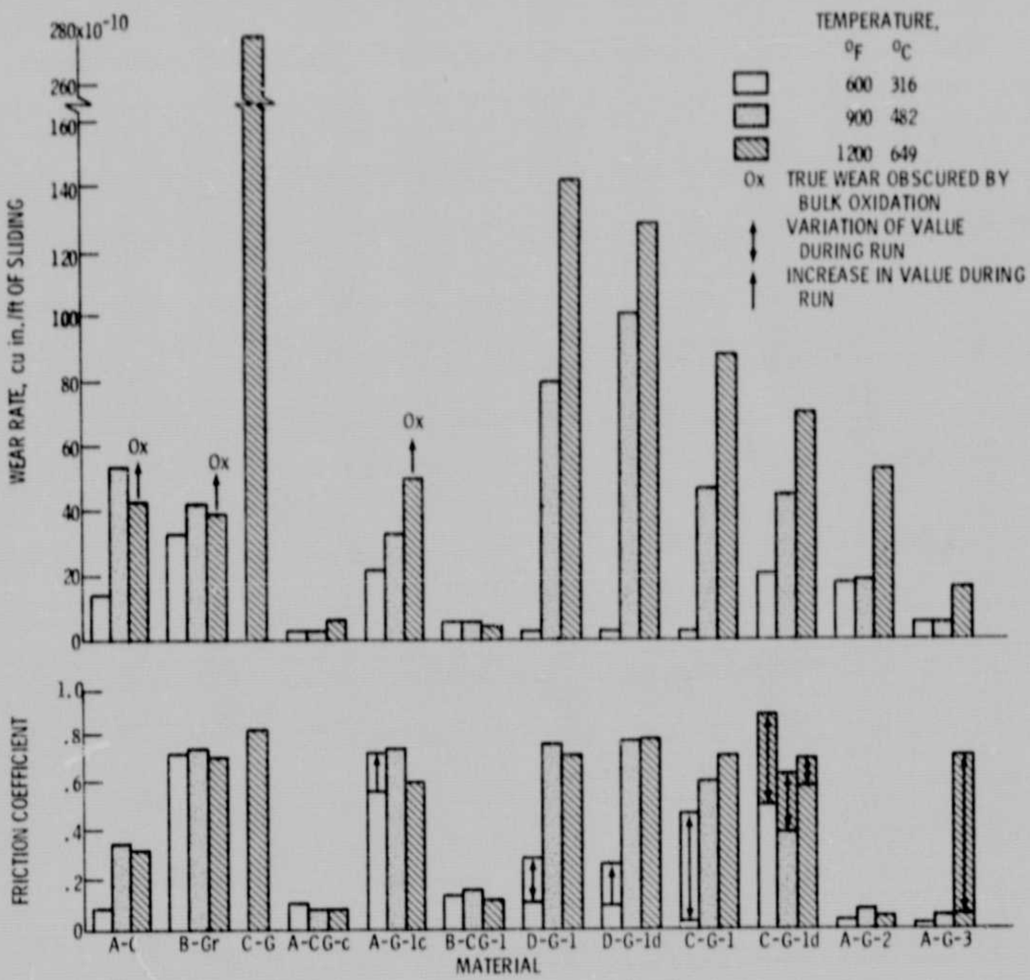

Figure 7. - Friction and wear of carbon-base materials sliding against chromium-plated nickel-base alloy.

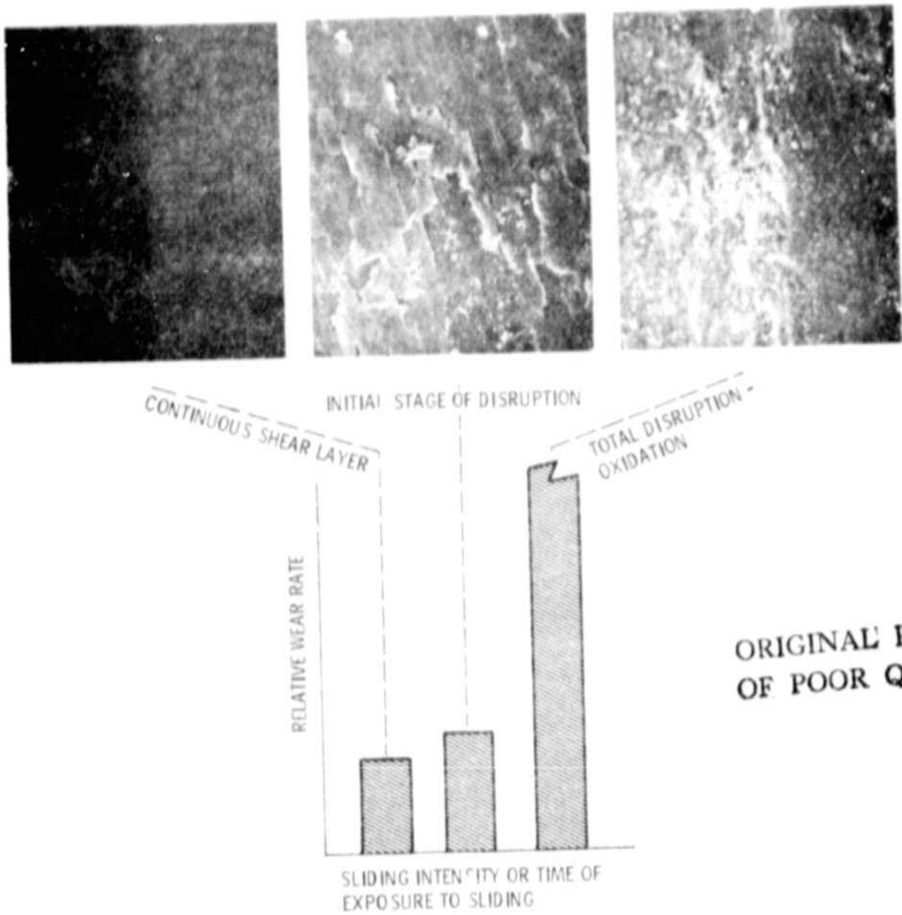

Fig. 8. - Three stages of shear layer transitions observed in sliding wear of carbon graphite.

Fig. 9. - Thermal cracking observed on contact surface of 440C face seal seat.

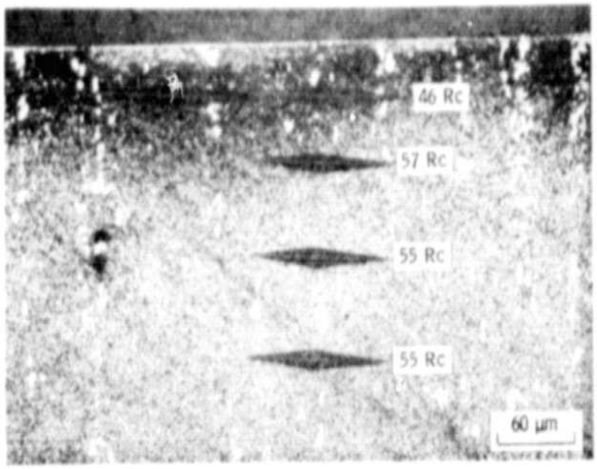

Fig. 10. - Metallographic section of 440C seal seat showing variation in hardness with depth below contact surface.

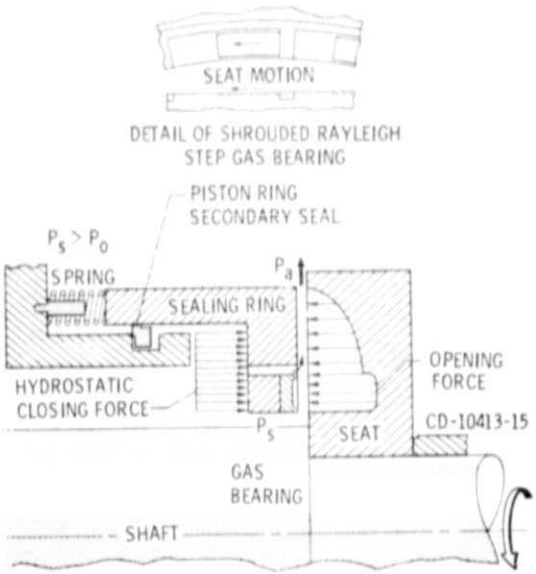

(a) SELF-ACTING LIFT PAD HYDRODYNAMIC SEAL.

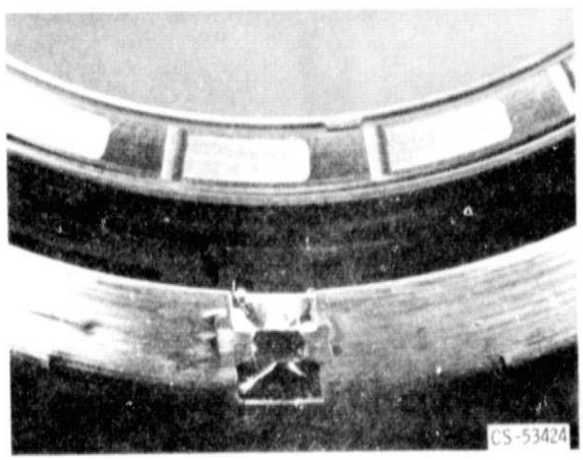

(b) PHOTOGRAPH OF SEAL RING SURFACE.

Figure 11. - Self-acting lift pad seal.

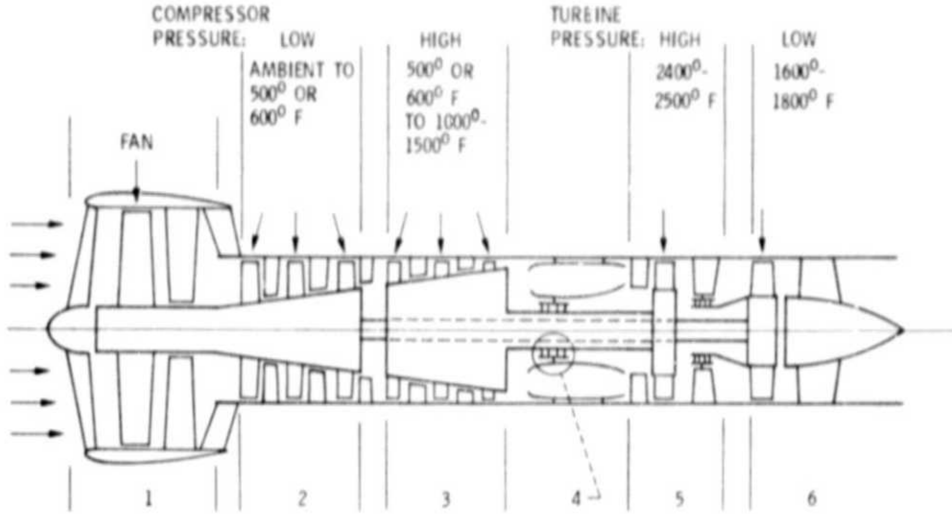

TYPICAL SEAL MATLS:

1 SILICONE RUBBER; Al HONEYCOMB; EPOXY
2 SPRAYED Al; SPRAYED NICKEL-GRAPHITE; SILICONE RUBBER; FIBERMETAL
3 HASTELLOY-X FIBERMETAL; SPRAYED NICKEL-GRAPHITE; SPRAYED NICHROME WITH ADDITIVES
4 LABYRINTH SEALS: Ag BRAZE; FIBERMETAL; HONEYCOMB
5 CAST SUPERALLOY (COOLED); SINTERED HIGH TEMP METALS; CERAMICS (EXPERIMENTAL)
6 SUPERALLOY HONEYCOMB

Figure 12. - Summary of engine operating environments and typical "abradable" seal materials.

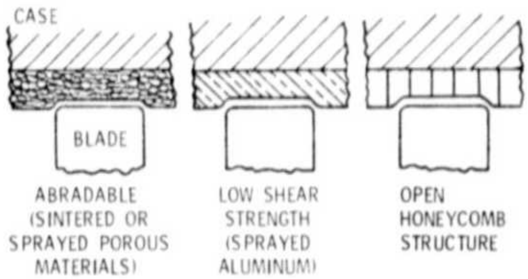

Figure 13. - Illustration of types of abradable seal materials for outer air sealing.

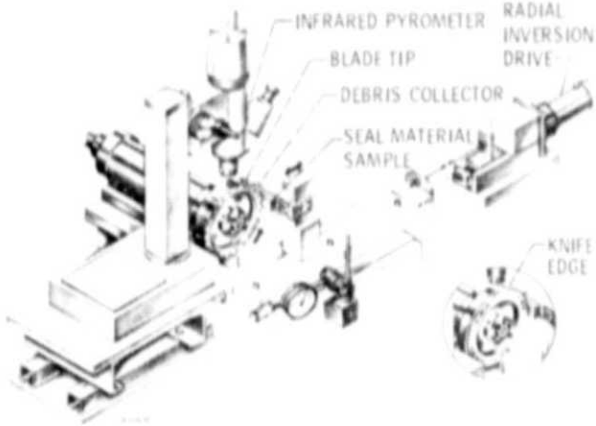

Figure 14. - ..st apparatus.

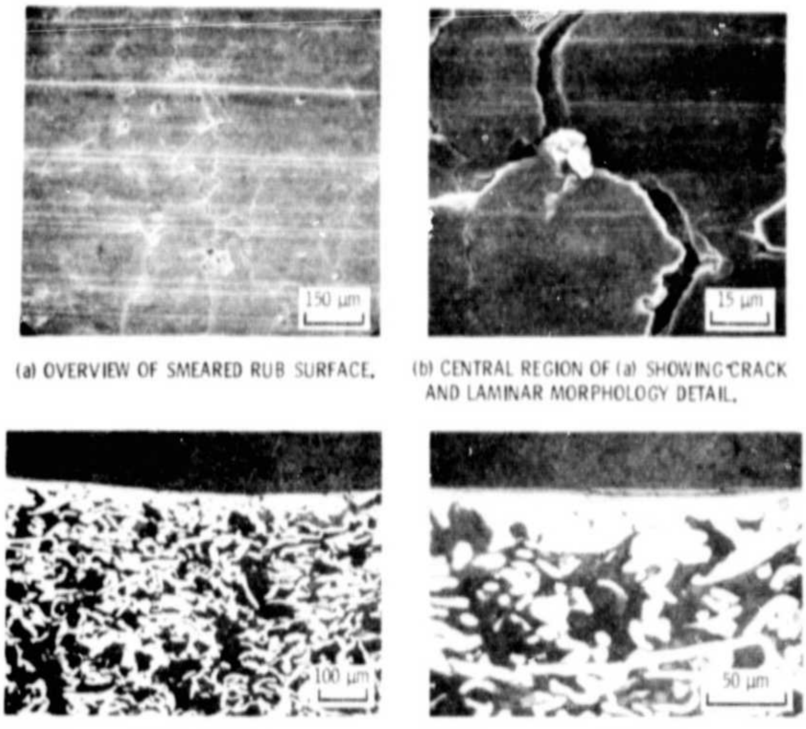

(a) OVERVIEW OF SMEARED RUB SURFACE.

(b) CENTRAL REGION OF (a) SHOWING CRACK AND LAMINAR MORPHOLOGY DETAIL.

(c) SECTION PARALLEL TO SLIDING DIRECTION, THROUGH SMEARED RUB SURFACE.

(d) DETAIL OF (c) SHOWING INCIDENCE OF LAMINAR CRACKS.

Fig. 15. - SEM overview and metallographic section of rub surface on sintered Hastelloy-X fiber-metal seal material after rub interaction with Ti-6Al-4V simulated blade tips.

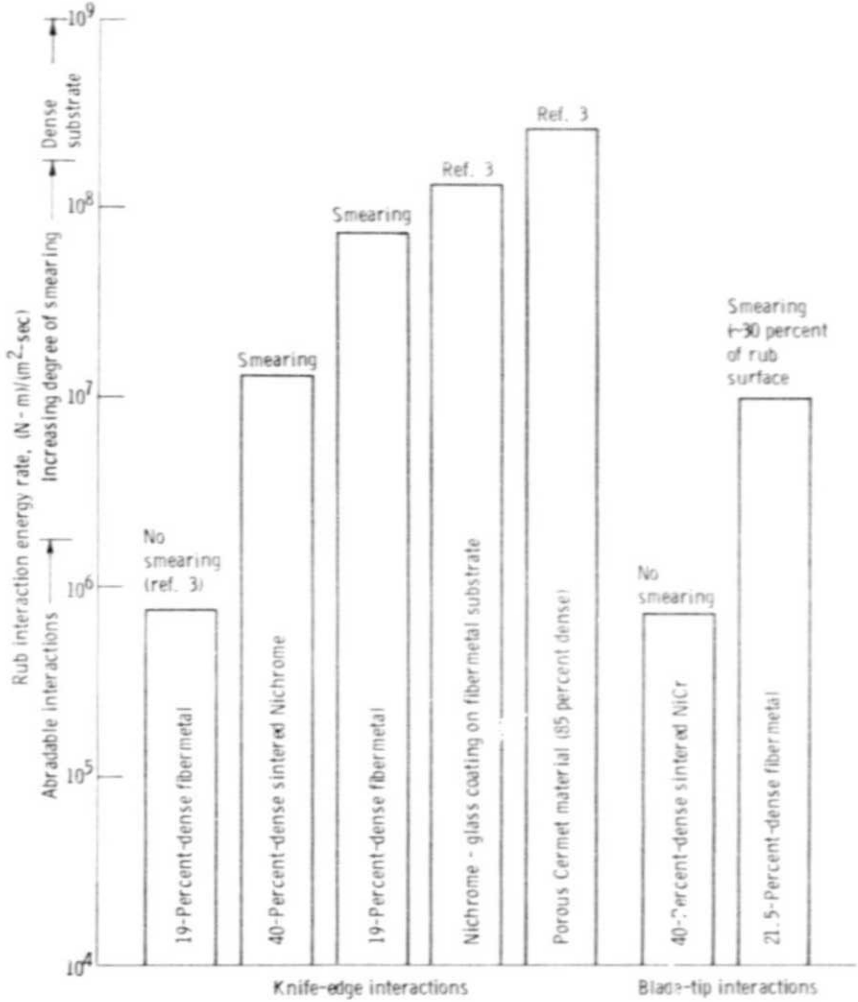

Figure 16. - Rub energy generation rate for various gas-path seal materials.

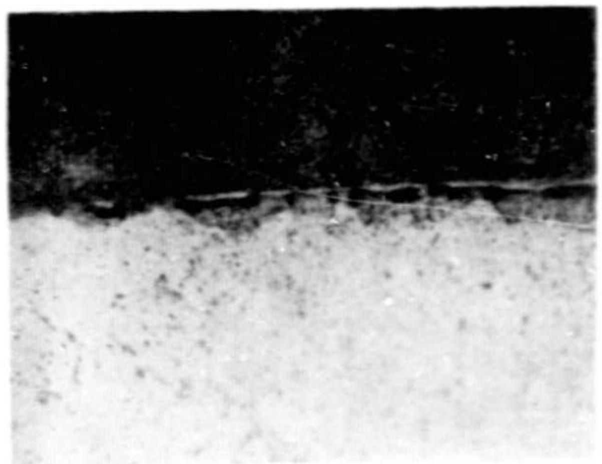

(a) NEAR BLADE-TIP LEADING EDGE.

(b) ABOUT HALFWAY ACROSS BLADE TIP.

Fig. 17. - Section view of Ti-6Al-4V simulated blade tip rub surface.

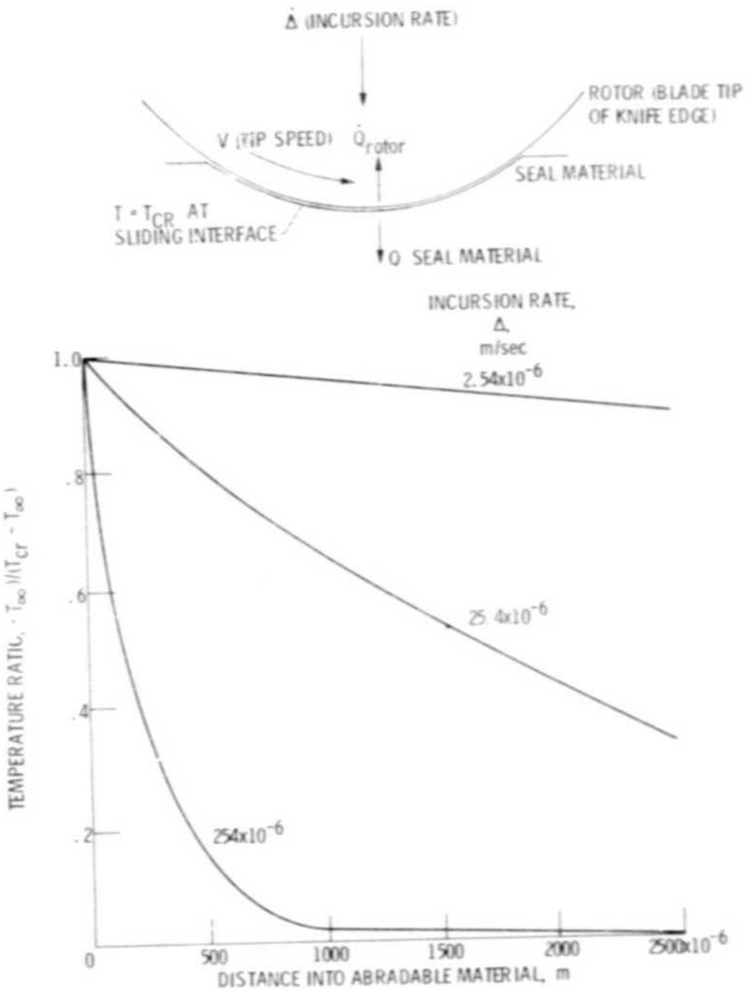

Figure 18. - Schematic representation of temperature profile beneath rub surface, in abradable material.

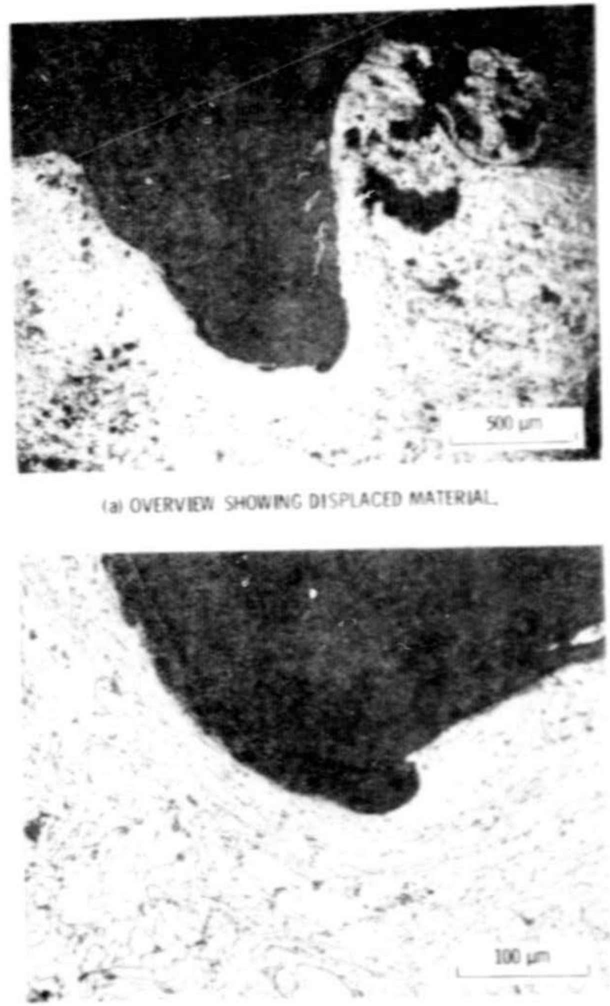

(a) OVERVIEW SHOWING DISPLACED MATERIAL.

(b) DETAIL, BOTTOM OF RUB GROOVE.

Fig. 19. - Microsection of rub groove on plasma-sprayed aluminum gas path seal material after interaction with 17 - 4 PH labyrinth seal knife-edge.

(a) RUB SURFACE ON PLASMA SPRAYED ALUMINUM.

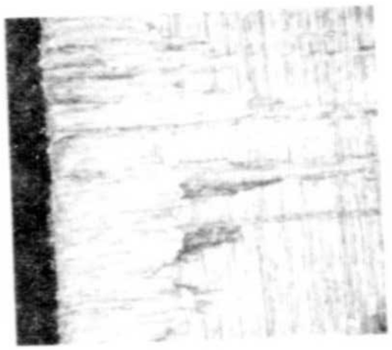

(b) Ti-6Al-4V BLADE-TIP LEADING EDGE SHOWING 20 MICROMETER A MINUM TRANSFER.

(c) WEAR DEBRIS IN FORM OF THIN TRANSLUSCENT RIBBONS.

Fig. 20. - Plasma-sprayed aluminum rub surface, Ti-6Al-4Vblade tip, and wear debris.

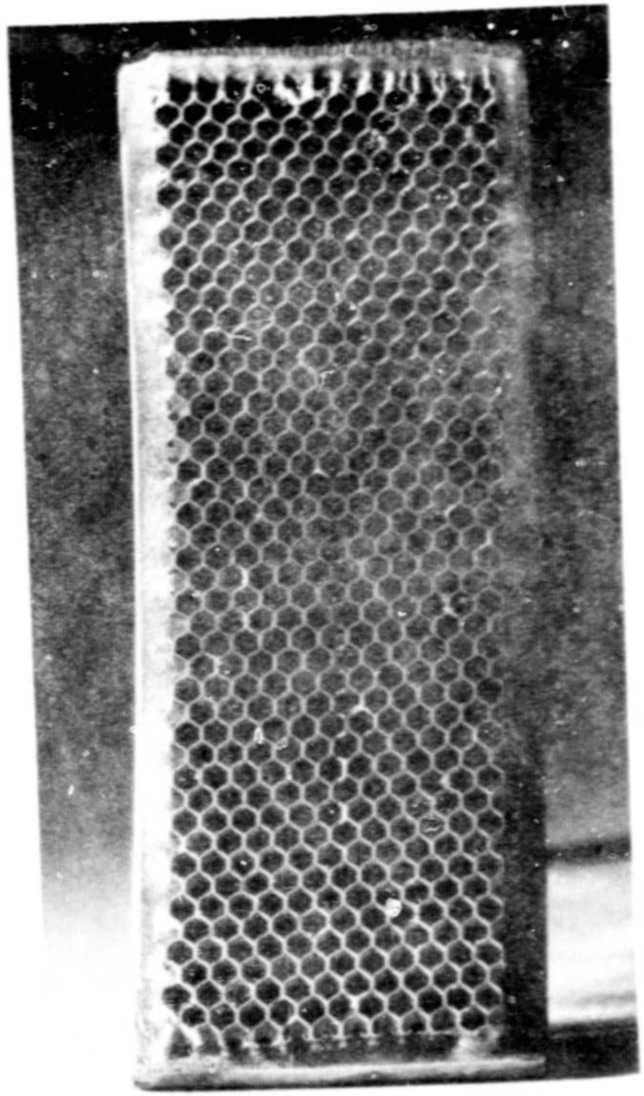

Fig. 21. - Seal surface of 1.6 mm (1/16") cell Hastelloy-X honeycomb.

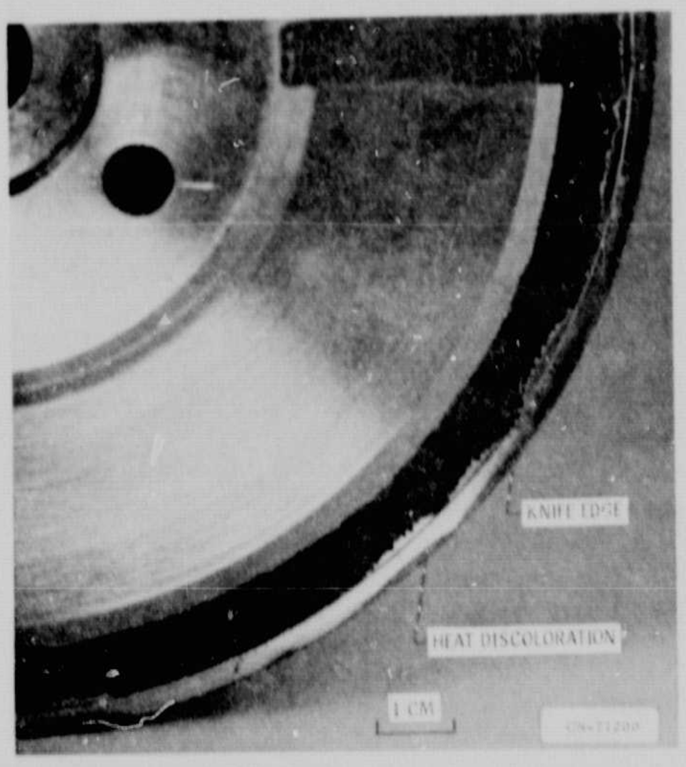

Fig. 22. - Labyrinth knife edge showing heat discoloration due to thermal bumps generated in rubbing contact against a honeycomb.